Away from generalized gradient approximation: orbital-dependent exchange-correlation functionals

Baerends, E.J.; Gritsenko, O.V.

published in
Journal of Chemical Physics
2005

DOI (link to publisher)
10.1063/1.1904566

document version
Publisher's PDF, also known as Version of record

Rotational effects in the dissociative adsorption of H_2 on the Pt(211) stepped surface

Marcello Luppi[a] and Drew A. McCormack
Theoretical Chemistry Department, Vrije Universiteit, 1081HV Amsterdam, The Netherlands

Roar A. Olsen
Leiden Institute of Chemistry, Gorlaeus Laboratories, Leiden University, P.O. Box 9502, 2300RA Leiden, The Netherlands

Evert Jan Baerends
Theoretical Chemistry Department, Vrije Universiteit, 1081HV Amsterdam, The Netherlands

(Received 20 May 2005; accepted 1 September 2005; published online 24 October 2005)

Rotational effects in the dissociative adsorption of H_2 on the Pt(211) stepped surface have been studied using classical trajectory calculations on a six-dimensional, density-functional theory potential-energy surface. Reaction of rotating molecules via an indirect trapping mechanism exhibits an unexpected nonmonotonic dependence on the initial rotational quantum number J. Indirect reaction is first quenched with increasing J but is enhanced again for high J initial states. The quenching is attributed to rotational-to-translational energy transfer, which facilitates escape from the chemisorption wells responsible for molecular trapping. For high J, rotational and translational motions decouple, and the energy transfer is no longer possible, which leads again to trapping. Degeneracy-resolved calculations show that for high initial J, molecules rotating in a "cartwheel" fashion ($m_J=0$) are more likely to become trapped and react indirectly than "helicoptering" molecules ($m_J=J$). Experimental confirmation of this finding would lend strong support to the existence of the chemisorption wells that trap molecules prior to reaction. © *2005 American Institute of Physics*. [DOI: 10.1063/1.2087467]

I. INTRODUCTION

Rough surfaces—which may include steps, kinks, defects, and/or facet edges—usually exhibit a strong enhancement of reactivity when compared to similar low-index single-crystal surfaces.[1–5] Despite a general acceptance that the rough features play a crucial role, the exact nature of the enhancement is not well understood.[6–8]

Recent experimental studies for hydrogen reacting on the Pt(533) surface have been enlightening as regards the mechanisms occurring in the dissociation of molecules on stepped surfaces.[9,10] The sticking probability was found to exhibit a nonmonotonic dependence on the collision energy of the impinging molecules, decreasing with increasing energy at low energies, and rising again at high energies. The authors were able to identify various direct and indirect reaction mechanisms by making some assumptions and fitting the data accordingly.

Partly motivated by these results, we recently presented the first theoretical studies on the dissociation of the H_2 molecule on Pt(211), which is a close relative of Pt(533). Our calculations utilized a six-dimensional (6D) density-functional theory (DFT) potential-energy surface (PES), the first full potential constructed for a diatomic molecule interacting with a stepped surface.[11] Using classical trajectories calculations, we reproduced the nonmonotonic dependence of the reaction on collision energy found in the experiments on Pt(533).

Our calculations showed that nonactivated sites atop the step atoms dominate the reaction. Direct reaction is found to occur at these sites at all energies. The amplification of reaction at low collision energies was also attributed to reaction atop the step atoms but not to any direct mechanism. Instead, molecules become trapped in shallow chemisorption wells at unreactive sites between the step and terrace. The time spent by these molecules near the surface increases the likelihood that they will migrate to the reactive upper edge of the step and dissociate.

In a second study we extended this work to include a more detailed analysis of high-energy reaction on the terrace and reaction at off-normal incidence.[12] This study showed that the trapping wells also play an important role in direct reaction when approaching at an angle to the surface normal, leading to a strong asymmetric dependence on incidence angle. Good quantitative agreement with the experiments on Pt(533) was found, and the experimental data reinterpreted in light of the calculations. In particular, we suggested that reaction atop the step was more important than originally thought, with the activated terrace sites playing a more minor role and only at high collision energies.

Though few studies have considered the effects of rotation on dissociation at stepped surfaces, many studies have dealt with flat surfaces. The Pd(111) surface, in particular,

[a]Electronic mail: luppi@few.vu.nl

which also exhibits a nonmonotonic dependence of reaction on collision energy, has been thoroughly investigated both theoretically and experimentally.[13–17]

Experiments have demonstrated a large reduction in the sticking coefficient for rotationally hot molecules.[13] It was suggested that this supported the existence of dynamical steering effects, because rotating molecules are less easily oriented by steering forces toward a geometry favorable for reaction.[13] The dependence of the sticking coefficient on the rotational state was advanced as a probe for distinguishing between precursor-mediated reaction and dynamical steering, in systems exhibiting an inverse dependence of sticking on beam energy.

However, more recent theoretical work of Busnengo *et al.* has shown that a precursor mechanism can also lead to a rotational suppression of reaction.[16] They found that dynamical trapping plays an important role in the dissociation of H_2 on Pd(111), promoting reaction at low collision energies. Using quantum and classical dynamics calculations, Busnengo has also found that for low rotational states, trapping is mainly due to translational (T)-to-rotational (R) energy transfer. High rotational states exhibit less trapping, but it does persist to some extent. For these states, trapping comes about as the result of energy transfer to parallel translational motion rather than rotation.

In this paper we present the results of calculations aimed at establishing the role of rotation in the dissociative adsorption of H_2 on Pt(211). This is the first study to make use of a 6D DFT PES in treating the effects of rotation on reaction for a stepped surface. Studying rotational effects can help us to identify new reaction mechanisms and suggest ways in which experiments could probe features of the PES.

Using classical trajectory calculations we have analyzed excited rotational initial states of hydrogen molecules up to $J=12$, including both degeneracy-averaged and degeneracy-resolved states. A detailed analysis of the 6D PES features and a new method for visualization of classical dynamics[12] have been used to identify reaction mechanisms.

In Sec. II we briefly detail the methods used to construct the PES, to perform classical dynamics calculations, and to analyze data. Section III presents results and discussion for rotationally excited hydrogen reacting on Pt(211), and Sec. IV concludes.

II. METHOD

A. H_2/Pt(211) 6D-PES construction

The electronic energy data points for the PES construction were obtained using the DFT program ADF-BAND.[18,19] The Kohn-Sham equations were solved self-consistently within a linear combination of atomic-orbital approach, modeling the surface by a slab with translational symmetry in two directions. A Becke-Perdew generalized gradient approximation (GGA) exchange-correlation functional was employed.[20,21] All aspects of these periodic DFT/GGA calculations are discussed in detail in Refs. 22–24.

To interpolate the DFT/GGA data, the corrugation-reducing procedure was employed.[25,26] This method has proven to provide very accurate interpolation results for H_2 molecules interacting with several metal surfaces.[25–30] The essence of the method is that the interpolation is not carried out on the highly corrugated DFT/GGA data itself but on the much smoother interpolation function obtained by first subtracting the separate atomic interactions with the surface. Details of the approach, and the interpolation techniques employed, can be found in Refs. 25 and 26.

More than 10 000 DFT/GGA data points were used in the PES construction. The resulting root-mean-square (maximal) error is around 20 (50) meV when tested against data points not included in building the PES.

B. Classical trajectory calculations

The dynamics have been studied by means of classical trajectory calculations. Although a rigorous treatment of rotational effects would require quantum mechanics, classical trajectories have been shown to adequately reproduce reaction dynamics of rotationally hot molecules in many systems, both activated[31–34] and nonactivated.[16,17,35] The classical approach has the advantage of being less computationally demanding and allows for easier physical interpretation of results; however, there are some drawbacks that must be considered.

One deficiency relates to the $J=1$ initial rotational state. Classically, the molecules in this state can rotationally deexcite, but quantally they may not scatter back with less rotational energy than the initial state, because for a homonuclear molecule such as H_2, odd transitions in J are forbidden. Although forbidden transitions can also impact the accuracy of classical results for higher rotational states, the error introduced tends to diminish with J as more rotationally deexcited channels open. Because of this issue, we focus little attention on results for $J=1$ throughout this paper.

Classical dynamics calculations were performed with 10 000 trajectories propagated for each initial state (unless stated otherwise). Microcanonical sampling was used, with each trajectory imparted a velocity toward the surface along the normal direction. Trajectories were initiated with no vibrational energy; such trajectories are usually called "classical trajectories," as opposed to "quasiclassical trajectories," which include quantum zero-point energy. Classical trajectories are known to behave better than quasiclassical trajectories for nonactivated systems.[16,36]

The initial rotational state of the molecules was set in one of the two ways. For degeneracy-averaged calculations, the angular momentum (L) of each molecule was chosen to give a rotational energy equal to that of the corresponding quantum state:

$$L = \hbar\sqrt{(J(J+1)I/I_{\mathrm{eq}}}, \tag{1}$$

where I is the moment of inertia of the molecule for the chosen geometry, and I_{eq} is the moment of inertia at the equilibrium geometry. After the atom velocities were adjusted, a random rigid rotation of the coordinates and velocities of the molecule was performed.

For degeneracy-resolved calculations, a vector model was utilized. The angular momentum was again set according to Eq. (1), but the molecular orientation was not chosen

randomly. Instead, beginning with the molecule parallel to the surface, three rotations were effected: First, a random rotation was performed about the surface normal; second, the system was rotated about an axis parallel to the surface and perpendicular to the molecular bond so that the angular momentum vector made an angle of $\arccos(m_J/\sqrt{J(J+1)})$ with the surface normal; and, last, another random rotation about the surface normal was performed. This sequence of rotations gives a molecular state consistent with the quantum angular momentum vector but otherwise random.

The fourth-order Runge-Kutta propagator was used to propagate the classical trajectories, with a time step of 5 a.u. Molecules were initiated with the bond center at a distance of $6.5a_0$ from the top of the step, as measured along the surface normal, and were evenly distributed in the surface plane. Trajectories were deemed to have reacted when their bond length exceeded $4.5a_0$ and were considered to have backscattered when the distance between bond center and step atoms exceeded $6.6a_0$, again measured along the surface normal.

C. Data analysis and visualization

In order to study the molecular trapping mechanisms the total reaction (or scattering) probability can be decomposed into its direct and indirect components. The measure of how directly each trajectory reacts (or scatters back) is based on the number of turning points a molecule undergoes perpendicular to the surface, i.e., in the Z coordinate, before it reacts (or scatters back). Direct reaction (or scattering) is considered to have occurred if the number of turns made is less than a given threshold, with all other trajectories being categorized as indirect. The choice of threshold is somewhat subjective. In Refs. 11 and 12 we have shown that a threshold of 6 represents a reasonable compromise because it gives a monotonically increasing component of direct reaction with collision energy, and a monotonically decreasing component of indirect reaction, dropping practically to zero at high energies. In this study, we adopt the same threshold. Although small quantitative changes could be expected to result from a different definition of trajectory directness, qualitative conclusions should not be affected.

Visualization is commonly used with classical dynamics to follow the evolution of individual trajectories in time. In this study, we make use of visualization techniques for whole ensembles of trajectories, which were developed in Refs. 11 and 12. In short, the discrete classical states at a given time are converted into a continuous spatial density by a fitting procedure, and a two-dimensional (2D) contour of the density is visualized as a function of time. The isosurfaces representing the density contour are in reality infinite in extent but in practice can be projected onto a single unit cell of the surface. With all trajectories initiated at the same distance from the surface, and evenly distributed in the surface plane, the isosurfaces are initially flat, with a finite separation arising from the fitting scheme. The regions of highest density are "sandwiched" between them.

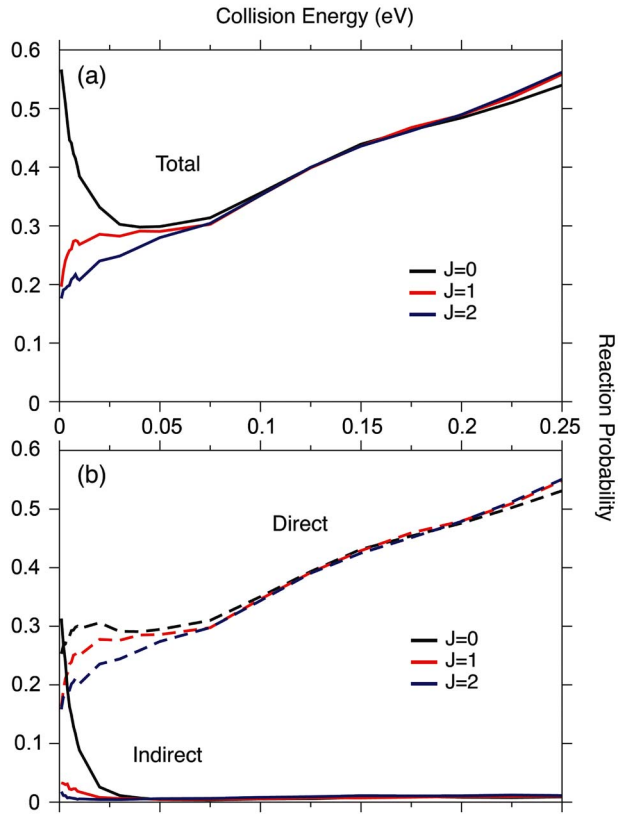

FIG. 1. Calculated reaction probabilities for low initial values of the rotational quantum number J and normal incidence. (a) Total reaction probability as a function of collision energy for $J=0$ (black), $J=1$ (red), and $J=2$ (blue). (b) Direct and indirect components of the total reaction probability as defined in Sec. II C for $J=0$, 1, 2 [the color scheme is the same as in (a)].

III. RESULTS AND DISCUSSION

A. Degeneracy-averaged results

1. Reaction probability versus collision energy: Low J

In Fig. 1(a) we compare the total reaction probability (RP) of normally incident molecules in the initial rotational states $J=0,1,2$. The curves are for degeneracy-averaged states and do not depend on the quantum number m_J. For the sake of the discussion we will divide the collision energy into two different ranges: low energy (LE) from 1 to 50 meV, and high energy (HE) from 50 to 250 meV.

The RP curve of the rotational ground state ($J=0$) displays a nonmonotonic dependence on collision energy, as shown by earlier studies.[11,12] The reaction decreases between 1 and 50 meV, almost halving in magnitude, and then begins to rise again.

Following the dynamics in time [Figs. 2(a)–2(c)], it becomes clear that the RP is made up of two components: a faster, direct (DIR) component, and a slower, indirect (IND) component [see Fig. 1(b)]. The DIR component has been shown to derive from two sources: nonactivated reaction at the top edge of the step, which is present over the entire range of energies, and activated reaction on the terrace, which only contributes significantly in the HE range.[12] The IND component is responsible for the inverse relationship

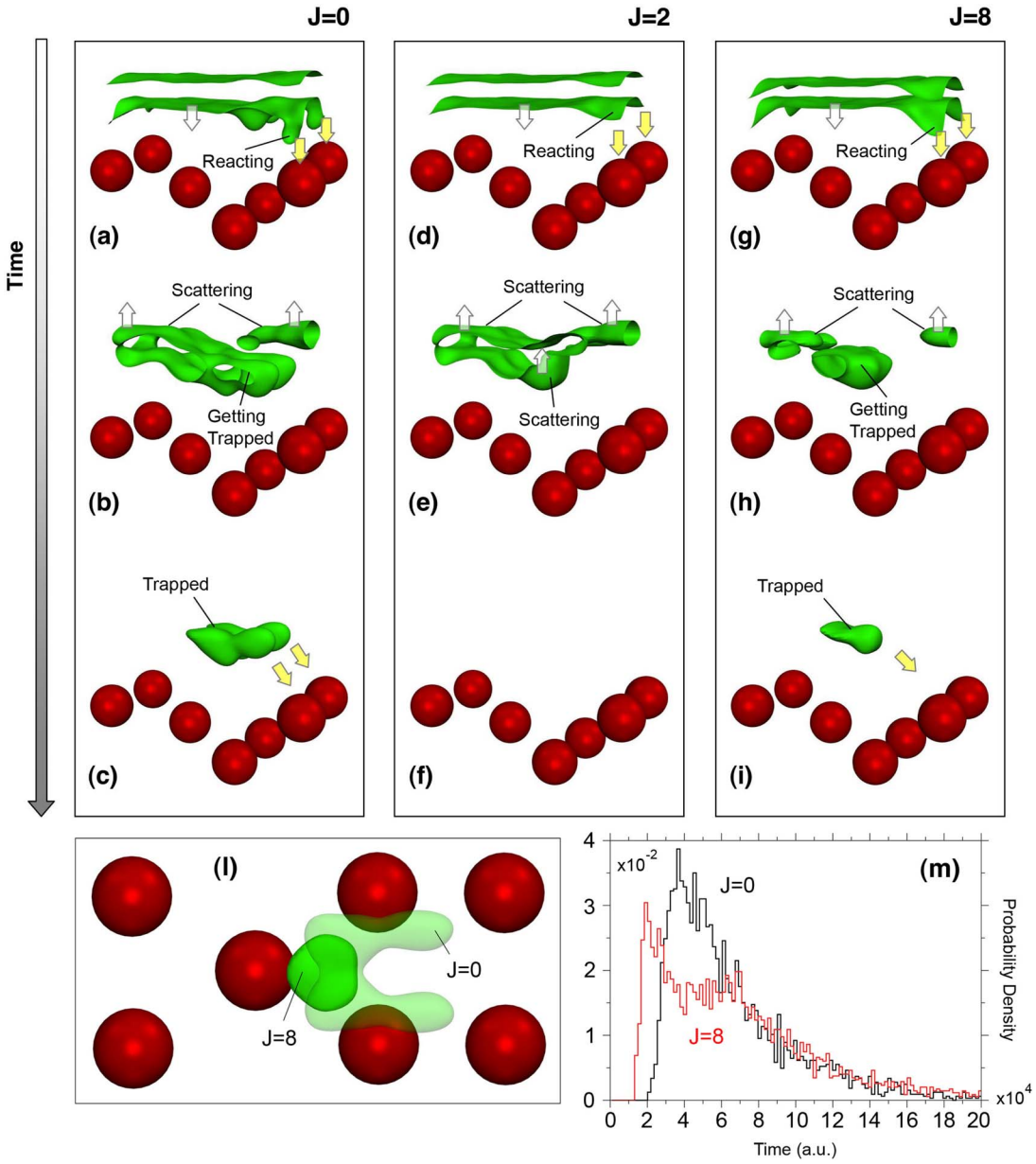

FIG. 2. (a)–(i) Visualization of the collective dynamics at 1 meV for three different initial rotational states: $J=0$, 2, 8. The green isosurfaces in each time frame represent the total density of molecules projected onto a single unit cell. (Ref. 12) The different frames for each J value correspond to different times, with time increasing down the page [e.g. from (a) to (c)]. The frames are not equally spaced in time. The white arrows indicate the motion of the total density isosurface, and the yellow arrows represent the motion of reacting trajectories. (l) Top view of the density of molecules for $J=0$ and $J=8$ after direct reaction is complete. The shape and location of the isosurfaces highlight the differences in the trapping region for the two initial rotational states. (m) Probability distribution of the lifetimes of reacting molecules for $J=0$ (black) and $J=8$ (red).

between reaction and collision energy in the LE range and has been attributed to dynamical trapping in a weak chemisorption well.[11,12]

In contrast to $J=0$, the RP of the $J=1$ and 2 initial rotational states simply increases monotonically with collision energy [Fig. 1(a)]. The enhancement of reaction seen for the rotational ground state at low energies vanishes when rotational motion is introduced. The natural conclusion of this would be that the trapping mechanism is quenched by rotation, and this is borne out in Fig. 1(b), which shows the IND component drops considerably in going from $J=0$ to $J=2$.

There are three different ways in which reaction via the trapping mechanism could be quenched:

- Molecules are scattered back directly while still far from the surface.
- Molecules reach the region responsible for trapping, but do not become trapped, and scatter back to the gas phase.
- Molecules do get trapped but scatter back rather than reacting.

In order to establish which mechanism is responsible for the quenching of reaction via trapping, we will now turn our focus to only those trajectories that begin above the trapping region and eventually scatter back to the gas phase. Reacting

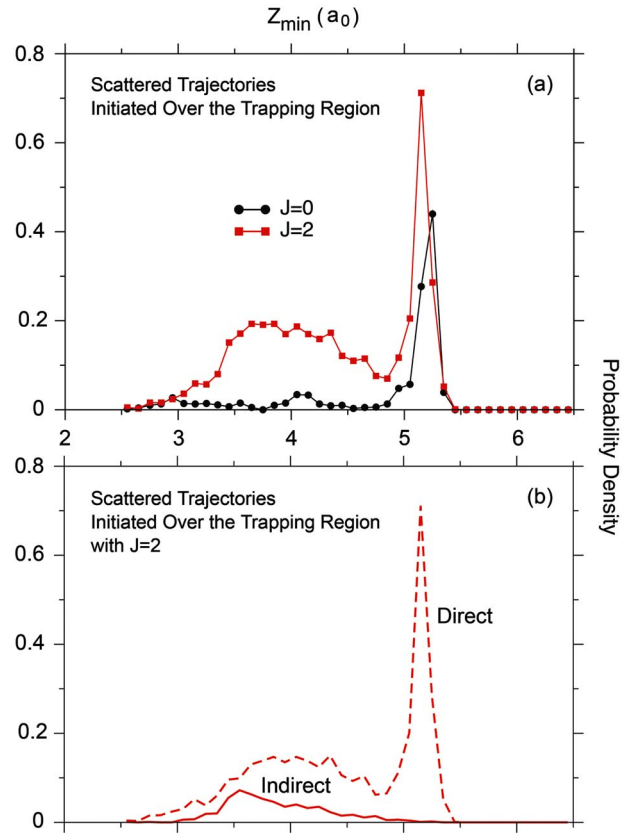

FIG. 3. (a) Probability distribution of scattered trajectories that begin above the trapping region. The behavior as a function of the shortest distance of approach to the surface is reported for $J=0$ (black dots) and $J=2$ (red squares) at the lowest collision energy sampled, 1 meV. The distributions are normalized to the total number of molecules. (b) Decomposition of the scattering probability plotted in (a) for $J=2$ into indirect (solid line) and direct (dashed line) components.

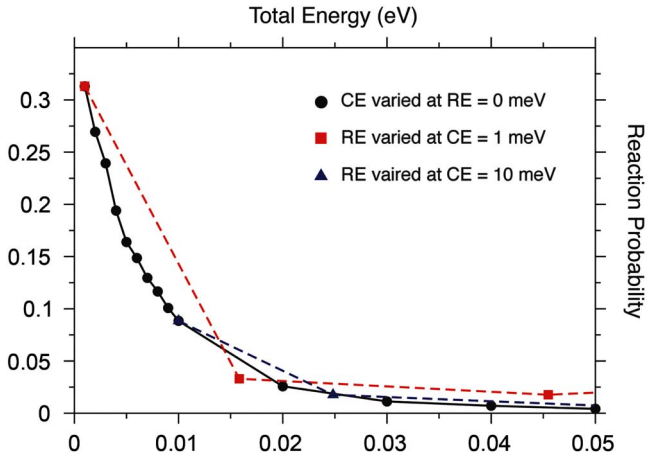

FIG. 4. Probability of reaction via the indirect mechanism as a function of the total energy. The black circles show the variation of the reactivity that results when the initial collision energy (CE) is varied for the initial rotational ground state. The other plots show the reactivity when the initial rotational energy (RE) is varied for a fixed collision energy. Plots are given for collision energies of 1 meV (red squares) and 10 meV (blue triangles).

trajectories, and trajectories beginning at other sites, are removed from the ensemble. The trapping region is defined for this purpose as in Refs. 11 and 12, namely, the region of the unit cell in the range of 5.0–10.5a_0 of the Y coordinate. Figure 3(a) shows the probability distribution of these trajectories as a function of the shortest distance of approach to the surface for the $J=0$ and 2 initial states at the lowest collision energy sampled (1 meV).

In the $J=0$ case the distribution shows a strong peak at around 5–5.5a_0 and almost no contribution at smaller distances. This means that nearly all scattering molecules scatter while still far from the surface. In the case of $J=2$, the number of scattered trajectories is larger than for $J=0$, as witnessed by the greater area beneath the $J=2$ curve (the area under each distribution integrates to the total scattering probability). The presence of a sharp peak similar to that for $J=0$ shows that there are still many molecules scattering at the beginning of their flight. The peak is somewhat larger than for $J=0$, but the increase is not dramatic enough to suggest that direct scattering far from the surface is responsible for the quenching of reaction seen at low collision energies.

The presence of a broadened peak in the distribution between $z_{min}=3a_0$ and 4.5a_0 shows that a large number of molecules scatter after having reached the trapping region of the PES. By separating the DIR and IND components [Fig. 3(b)], we have also established that the majority of the trajectories that visit the trapping region never become trapped but are scattered directly. The reduced reactivity of the $J=2$ initial state at low collision energies thus comes about because molecules entering the potential wells are not trapped as they are for $J=0$ and thus cannot react via the precursor mechanism. This picture is well supported by the time evolution of the density of molecules for $J=2$ plotted in Fig. 2(d)–2(f) compared to the $J=0$ case [Figs. 2(a)–2(c)].

The question then arises of why the $J=2$ molecules do not become trapped. We attribute this to coupling between the translational and rotational degrees of freedom in the trapping region. At the low energies for which trapping occurs (<50 meV), a $J=1$ or 2 molecule has a rotational energy (E_{rot}) comparable to its initial translational (collision) energy: for $J=1$ E_{rot} is 15 meV, and for $J=2$ it is 45 meV. The time scales of the rotational and translational motions are thus comparable, and a rotational-to-translational ($R \rightarrow T$) transfer of energy likely, due to the anisotropy of the PES in the trapping wells. Rotational energy can find its way into the translational motion away from the surface and allow the molecules to escape.

Evidence for this mechanism can be found in the influence that changing the initial rotation and translation has on the RP. The total energy of an incident molecule can be changed by fixing its rotational energy, and varying its translational energy; or by keeping the translational energy fixed, and varying the initial rotational state. By plotting the reaction probability obtained in each case versus the total energy, we can compare the influence of each motion on dissociation.

Figure 4 shows these results for the IND component of the RP. By comparing the curves in Fig. 4 at different total energies, it is evident that the two motions are almost equally effective at quenching reaction. It does not matter which channel energy is initially added to, the impact on IND re-

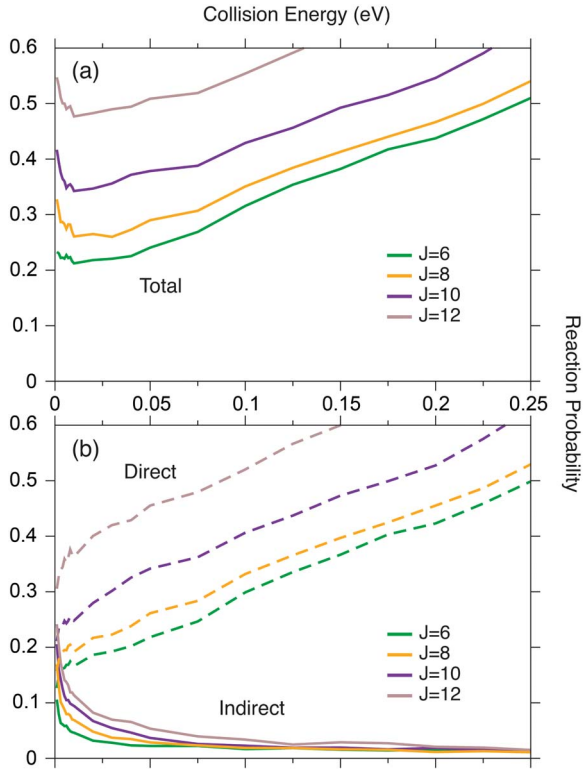

FIG. 5. Calculated reaction probabilities for high initial values of the quantum number J and normal incidence. (a) Total reaction probability as a function of the initial collision energy for $J=6$ (green), $J=8$ (orange), $J=10$ (violet), and $J=12$ (brown). (b) Direct and indirect components of the reaction probability as defined in Refs. 11 and 12 for $J=6$, 8, 10, 12 [the color scheme is the same used in (a)].

action is similar. This suggests that energy can be efficiently transferred from rotation to translation in the trapping wells.

To this point we have focused on the LE range. At high collision energies, the RP shows very little dependence on J for $J=0$, 1, 2. The three curves in Fig. 1(a) are virtually identical between 75 and 250 meV. This can be explained using another time scale argument. At these collision energies, the time scale of translational motion is shorter than that of rotation for slow-rotating molecules. Molecules incident with $J=1$ or 2 can thus be considered nonrotating from the perspective of dissociation.

2. Reaction probability versus collision energy: High J

Figure 5 shows the RP of faster-rotating molecules ($6 \leqslant J \leqslant 12$). The enhancement of reaction in the LE range, which characterizes $J=0$ trajectories, but is absent for the $J=1$ and 2 states, reappears for the high-lying initial rotational states. The curves exhibit an inverse dependence of reaction on collision energy in the LE range. They also shift upwards with increasing J.

Following the dynamics in time [Figs. 2(g)–2(i)], we again identify a direct component of reaction on the atop site of the step [Fig. 2(g)] and an indirect component reacting via the trapping region at the lower edge of the step [Fig. 2(i)]. The enhancement of reaction in the LE range is due to the indirect trapping mechanism, as demonstrated by the IND-RP plots in Fig. 5(b).

The nature of trapping for high-J initial states differs somewhat from that for $J=0$. This is clearly evident in Fig. 2(l), which shows that the region occupied by trapped molecules is different for $J=0$ and $J=8$. The trapping lifetime is similar though, as seen in Fig. 2(m). While direct reaction proceeds faster for $J=8$ than $J=0$, as evidenced by the position of the first peak in each distribution, the tail of the distribution, which corresponds to indirect reaction, is similar for the two initial rotational states.

For low collision energies, the time scale of rotation is much shorter than that of translation. The two motions are effectively decoupled, with little energy transfer between them. This is demonstrated in Fig. 6. Panel (a) shows the probability distribution of the scattered trajectories as a function of the value of $J(J+1)$ upon scattering [the value of $J(J+1)$ is proportional to the rotational energy]. The absence of any significant broadening in the distribution indicates that the molecules scatter elastically with respect to the J quantum number, with very little transfer to other motions such as translation. Panel (b) reports the averaged rotational energy (green dots) of trapped molecules as a function of time. The absence of significant fluctuations in the rotational energy demonstrates that rotational motion is largely decoupled from other degrees of freedom.

Given the differences in time scale, it is not unreason-

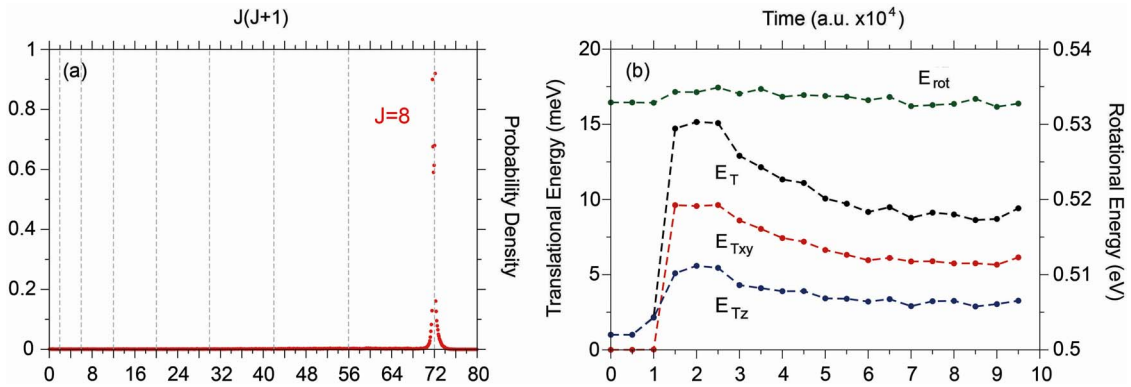

FIG. 6. Behavior of trajectories initiated in the $J=8$ state (high J) with collision energy of 1 meV (ensemble of 100 000 trajectories). (a) Probability distribution of scattered trajectories as a function of the final $J(J+1)$ value. (b) Time evolution of translational and rotational energies of trapped molecules. Two energy scales have been used, one for translation (left end, meV) and one for rotation (right end, eV). The averaged total translational energy (E_T) is represented by black dots, the parallel ($E_{T_{xy}}$) and perpendicular (E_{T_z}) components by red and blue dots, respectively, and the averaged rotational energy (E_{rot}) by green dots.

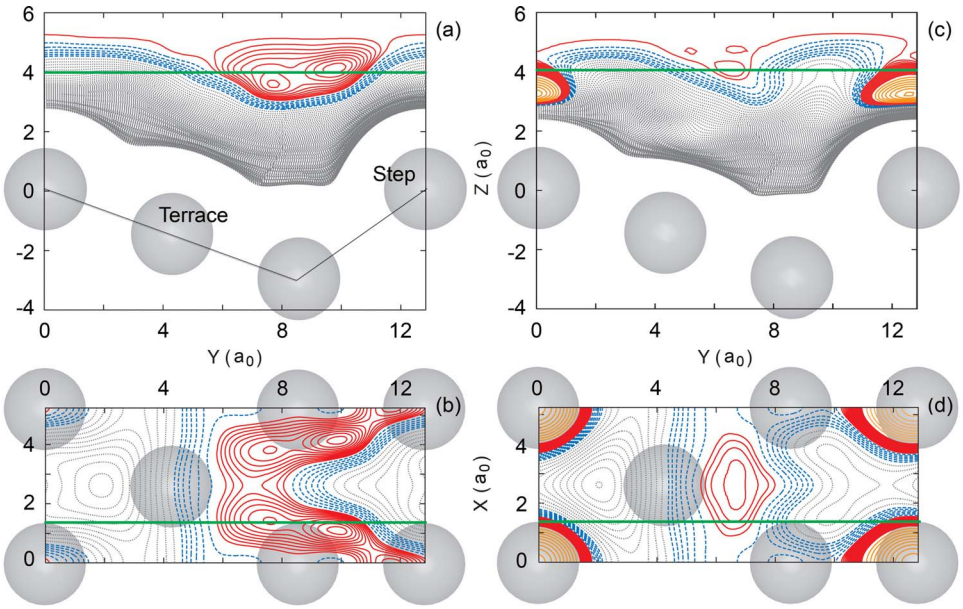

FIG. 7. Effective potential-energy surfaces for fast-rotating molecules. Contour plots for various two-dimensional (2D) cuts are reported. The Pt atoms of the unit cell are represented by the gray spheres, and are shown from above in (b) and (d), and from the side in (a) and (c). The green line in (a) and (c) shows the position of the *XY* cut plotted in (b) and (d), while the green line in (b) and (d) indicates the location of the *YZ* cut used in (a) and (c). (a) and (b) are for an effective PES in which the molecular axis is kept in the *YZ* plane, and an average is taken over the polar angle θ. (c) and (d) are for an effective PES averaged over the azimuthal angle ϕ, with the molecule parallel to the (211) surface. In both cases, the H_2 bond length is constrained to the gas-phase equilibrium value. Contours between 5 and 30 meV (dashed blue lines), relative to the gas-phase minimum, are at intervals of 5 meV; those from 40 to 1.04 eV (dotted gray lines) are at intervals of 10 meV; those from 0 down to −38 meV (solid red lines) are at intervals of 2 meV; and those from −40 down to −1.23 eV (solid orange lines) are at intervals of 10 meV.

able to consider the rotational motion as evolving adiabatically, with the translational motion determined by an orientationally averaged potential. For example, the translational motion of a molecule approaching the surface with its angular momentum vector normal to the surface (so-called "helicoptering" motion) is governed approximately by an effective potential generated by averaging the 6D PES over the angle ϕ, the azimuthal angle that defines the orientation of the molecular axis in the (211) surface plane.

In Fig. 7 we present several contour plots of orientationally averaged PESs. The plots show that the averaged PESs exhibit shallow wells where trapping can occur for certain angular momenta. But given that $T \rightarrow R$ energy transfer is virtually forbidden, how does this trapping come about? The fast-rotating molecules can still transfer energy from translation perpendicular to the surface, to motion parallel to the surface, and become trapped in the process. This is clearly shown in Fig. 6(b). The averaged total kinetic energy (E_T), for molecules in the $J=8$ state and with an initial collision energy of 1 meV, is plotted as a function of time together with the components in the surface plane ($E_{T,xy}$) and along the normal to the surface (E_{T_z}). The growth of $E_{T,xy}$, which is initially zero, indicates that for molecules entering the potential wells, around two-thirds of the available kinetic energy ends up in translational motion parallel to the surface. This energy must be reconcentrated into the perpendicular translational mode if escape back to the gas phase is to take place. Molecules thus become trapped due to a transfer of energy into the parallel translations.

Reaction in the LE range is enhanced by increasing J from 6 to 10. This is partially attributable to an increase in the indirect component with increasing J [Fig. 5(b)]. There are two ways that this increase could come about:

- Increasing J produces an increase of the probability of trapping, leading to greater reaction as a result.
- The conditional probability of a trapped molecule reacting increases with J, i.e., once trapped, a molecule is more likely to react.

The probability of trapping for different initial rotational states is shown in Fig. 8(a). The higher the initial value of J, the more likely the molecules are to become trapped. This may be because the translational and rotational motions become more decoupled as J is increased, and $R \rightarrow T$ energy transfer becomes less likely, which further decreases the likelihood that rotational energy can be used to escape the trapping wells.

The conditional probabilities of a molecule reacting after it has become trapped are given in Fig. 8(b). Results are for collision energies of 1, 5, and 10 meV and are shown as a function of initial J. After an initial drop at low J, the conditional probability rises with increasing J, indicating that faster-rotating molecules have a greater chance of reacting once they have become trapped. So the increase in indirect reaction with initial rotational state (J) is a result of both an increase of the probability of becoming trapped and an increase in the probability of a molecule reacting once trapped.

The growth of the conditional probability with J could also come about in a couple of different ways:

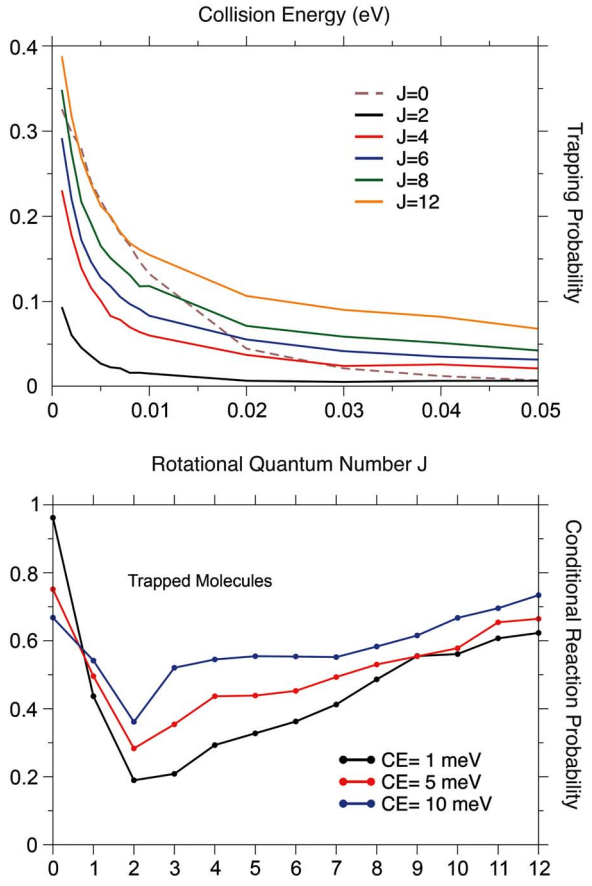

FIG. 8. (a) Trapping probability as a function of the collision energy for different initial J values: $J=0$ (brown-dashed), $J=2$ (black), $J=4$ (red), $J=6$ (blue), $J=8$ (green), and $J=12$ (orange). (b) Conditional reaction probability of trapped molecules (i.e., probability of reacting once trapped) as a function of the rotational quantum number J for three different collision energies: 1 meV (black), 5 meV (red), and 10 meV (blue).

- The trapping of molecules with higher J could be longer in duration, giving more opportunities to react.
- Reaction is enhanced by the rotational energy of higher J states.

In the latter, rotational energy could be transferred to the dissociative mode via a rotationally adiabatic process as the molecular bond extends. Due to the high rotational energy available, only small extensions of the bond are needed to result in considerable energy transfer.

To distinguish between these possibilities, we have considered trajectory lifetimes for different initial J states and find no evidence of longer residence times for high-J molecules. We therefore tentatively ascribe the increase in conditional probability with initial J to rotationally adiabatic energy transfer.

Note that this mechanism does not imply any deexcitation of rotation; the energy of the rotational state decreases adiabatically as the bond extends. A kinetic-energy coupling transfers energy from the rotational degrees of freedom to the dissociative bond-stretching mode. This does not contradict the earlier claim that rotation and translation are largely decoupled in the trapping region for high rotational states, because the coupling in that instance is a potential coupling, which leads to the excitation or deexcitation of the rotational-librational state of the molecule. The kinetic-energy coupling that leads to adiabatic energy transfer can aid reaction of trapped molecules, but it cannot help molecules escape the trapping well and return to the gas phase, because that would require the bond length of a scattered molecule to differ from that of an incident molecule.

It is widely accepted that rotationally adiabatic transfer is responsible for the enhancement of direct reaction with J that is generally seen for J greater than approximately 6 and which is also observed in this study [Fig. 5(a)].[16,32,37–39] In the HE range, the dissociation is predominantly direct in nature, while in the LE range the direct and indirect components both contribute [Fig. 5(b)]. The adiabatic enhancement affects the direct components on both the step and terrace sites, as well as enhancing the indirect component, as shown above.

A measure of the rotationally adiabatic enhancement is given by the relative efficacy of rotation with respect to translation, which we have determined is around 15% in this case. The relative ineffectiveness of rotation in enhancing reaction can be attributed to the fact that reaction is nonactivated at the reactive step sites, and that there is an early barrier at the most reactive site on the terrace. For nonactivated sites rotation plays a minor role in reaction, and an early barrier means there is little bond extension of incident molecules, and thus less energy transfer from rotation to the dissociative mode.

3. Reaction probability versus J

Figure 9 presents the RP as a function of initial J for various collision energies. In the HE range (i.e., 150 and 250 meV), where the DIR component dominates, the RP first decreases with J, reaches a minimum at around $J=5$ or 6, and then rises again. This behavior has been observed for many activated and nonactivated dissociation reactions on flat metal surfaces.[16,17,37,38,40–43]

The phenomenon was explained first by Darling and Holloway.[37] The initial drop can be ascribed to rotational shadowing (hindering). In a direct reaction, a rotating molecule is more likely to be in an unfavorable geometry for reaction at some point in its approach to the surface and is thus more likely to be scattered. For higher rotational states, the rotationally adiabatic exchange of energy discussed earlier begins to dominate, and reaction begins to increase with J.

The IND component experiences a sudden drop of RP between $J=0$ and $J=1$ [Fig. 9(c)]; this is due to the $R \rightarrow T$ energy transfer discussed earlier, which quenches trapping. For faster-rotating molecules, the potential coupling between rotation and translation becomes small, and trapping resumes. This leads to the increase of the IND-RP curves at higher-J values.

B. Degeneracy-resolved results

1. Dependence of reaction on rotational orientation

Figure 10 compares the reaction probabilities of molecules initiated in the so-called helicopter ($m_J=J$) and cart-

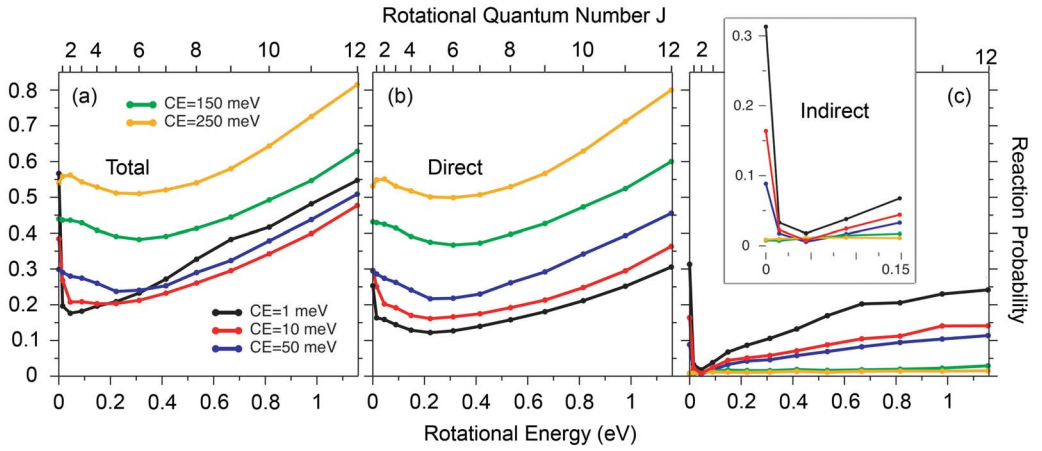

FIG. 9. Reaction probabilities as a function of initial J: (a) total reaction probability; (b) and (c) direct and indirect components of reaction. Results for different collision energies are reported: 1 meV (black), 10 meV (red), 50 meV (blue), 150 meV (green), and 250 meV (orange). The inset in (c) shows the low-energy range in greater detail.

wheel (m_J=0) states. In the helicopter state (a), where molecules rotate almost parallel to the (211) surface plane, the RP grows with J at all collision energies. This is consistent with an enhancement of reaction due to rotationally adiabatic energy transfer to the dissociative mode.

Reaction curves for the cartwheeling molecules first decrease with $J(J \leqslant 6)$ and then begin to rise again. This is due to the rotational hindering described above. Rotational hindering arises when a molecule encounters a strong anisotropy in the PES as it rotates, and cartwheeling molecules do tend to sample a wide range of potentials. The helicoptering states do not exhibit rotational hindering, because the PES is much more isotropic for rotation parallel to the surface.

The enhancement of reaction at low collision energies going from J=8 to J=12 is greater for cartwheel states than helicopter states [Figs. 10(a) and 10(b)]. This can be attributed to the cartwheel state reacting more via the indirect mechanism than the helicopter state. Figure 10(c) shows the

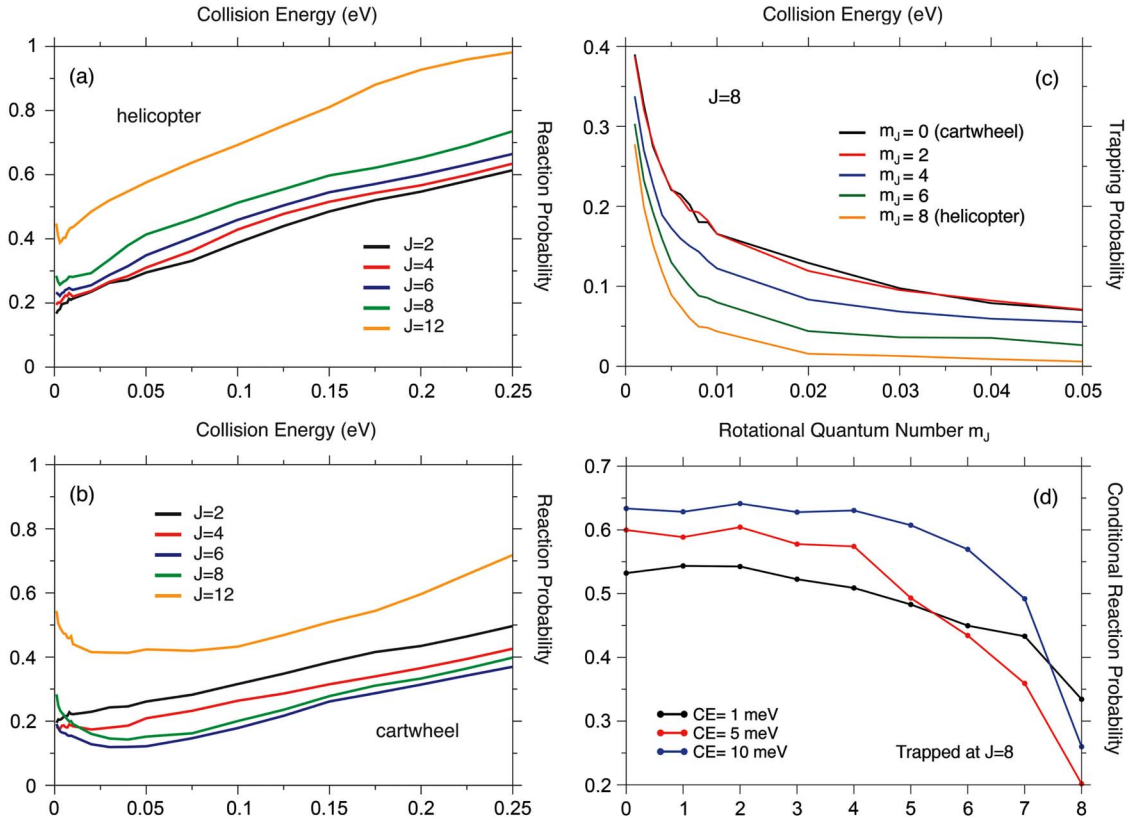

FIG. 10. (a) and (b) Reaction probability as a function of collision energy for different degeneracy-resolved rotational states. Panel (a) presents results for trajectories with m_J=J (i.e., helicopter), and panel (b) presents results for trajectories with m_J=0 (i.e., cartwheel). Results are given for J=2 (black), J=4 (red), J=6 (blue), J=8 (green), and J=12 (orange). (c) Trapping probability as a function of collision energy for J=8 with m_J=0 (black), m_J=2 (red), m_J=4 (blue), m_J=6 (green), and m_J=8 (orange). (d) Conditional reaction probability of trapped molecules for J=8 as a function of m_J for three different collision energies: 1 meV (black), 5 meV (red), and 10 meV (blue).

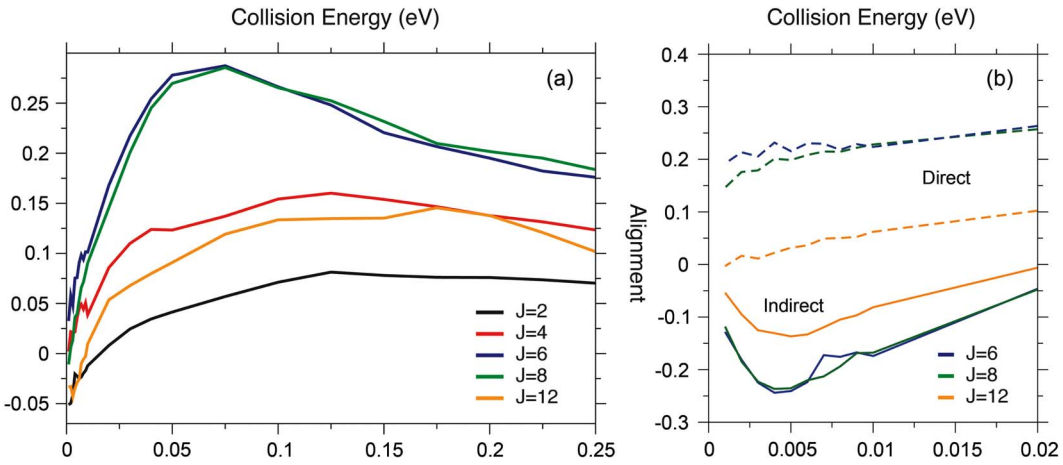

FIG. 11. (a) Calculated quadrupole alignment [see Eq. (2)] as a function of the initial collision energy for different rotational states: $J=2$ (black), $J=4$ (red), $J=6$ (blue), $J=8$ (green), and $J=12$ (orange). (b) Separate alignments of directly (dashed lines) and indirectly (solid lines) reacting molecules for $J=6$ (blue), $J=8$ (green), and $J=12$ (orange).

probability of molecules becoming trapped for various m_J states with $J=8$; the cartwheel state ($m_J=0$) has the greatest chance of trapping, and the helicopter ($m_J=J$) the least. Not only is the probability of trapping greater for the cartwheel but the probability of reacting once trapped is also greater, as shown in Fig. 10(d).

This behavior can be understood by considering the orientationally averaged contour plots in Fig. 7. The trapping wells for a cartwheeling molecule are similar in shape to those in the full 6D PES,[11,12] with two lobes extending from the bottom edge of the step to the reactive top of the step. The trapping region for a molecule rotating parallel to the surface is shifted more towards the terrace and does not extend to the reactive top sites. The depth of the well in the helicopter-averaged PES is also less than for cartwheeling molecules.

These aspects of the rotationally average PESs help us to interpret the findings above. Cartwheel molecules are more likely to become trapped, because the wells for these molecules are deeper. Once trapped, they are also more likely to react, because they are free to move into the vicinity of the reactive step sites. Helicopter molecules are not only less likely to become trapped but are also less likely to react once trapped, because they cannot approach the step. In order to react, a trapped helicoptering molecule would need to begin rotating in a more cartwheel fashion.

These results show that for fast-rotating molecules the enhancement of reactivity at low collision energies is largely due to molecules that rotate out of the plane of the surface. This is one example of the profound influence that surface steps can have on reaction dynamics.

Svensson *et al.* have reported the existence of a rotationally constrained molecular chemisorption state on a stepped copper surface.[44] Taken together with our findings, these results suggest that molecular chemisorption states with a strong rotational bias may be a common feature of molecular interactions at surface steps, which is of relevance to the construction of molecular-scale machines and devices.[45–50]

2. Alignment

The quadrupole alignment is a measure of the preferred rotational orientation of reacting molecules. It is an important quantity because it can be measured in associative desorption experiments,[51] allowing for direct comparison with the results of calculations. The quadrupole alignment parameter is defined as $A_J^{(2)}(E)=\langle 3\cos^2\Theta-1\rangle$, where Θ is the angle between the angular momentum vector and the surface normal.

It can be shown that the alignment is equal to

$$A_J^2(E)=\frac{\sum_{m_J} P(E;J,m_J)[3m_J^2-J(J+1)]/J(J+1)}{\sum_{m_J} P(E;J,m_J)}, \qquad (2)$$

where $P(E;J,m_J)$ is the reaction probability at collision energy E. The lower limit on the alignment is always -1, which corresponds to the case where only the cartwheel state ($m_J=0$) reacts. The upper limit increases with J, asymptotically going to 2. The upper limit is attained if the only reacting molecules are in the helicopter state ($m_J=J$). An alignment of zero results if reaction is equally likely for all m_J states.

In Fig. 11(a) we compare the collision energy dependence of $A_J^{(2)}$ for various initial rotational states. A nonmonotonic dependence is observed for all the states: First the alignment increases and then gradually declines. The alignment tends to increase going from $J=2$ to $J=8$ and decrease between $J=8$ and $J=12$. The J dependence can be explained by the results presented earlier. The increase in alignment with J arises because helicoptering molecules become more reactive due to rotationally adiabatic energy transfer, while the cartwheeling molecules actually become less reactive due to rotational hindering. For higher-J states, adiabatic enhancement also begins to dominate for the cartwheel state, and the alignment decreases accordingly. Similar findings have recently been reported by Busnengo *et al.*[16]

The alignment of the high-J states becomes zero and even negative at very low collision energies, indicating that out-of-plane rotation is actually preferred for reaction over

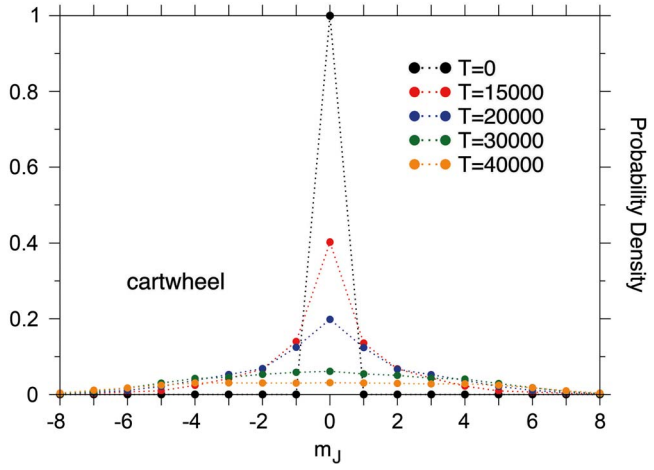

FIG. 12. Probability distribution of m_J values at five different times for indirectly reacting molecules initially in the (J=8, m_J=0) state.

in-plane rotation. This is due for the most part to the indirect trapping mechanism [Fig. 11(b)], which favors reaction of cartwheel states. This unusual preference for out-of-plane rotation is a direct consequence of the steps in the surface, and experimental measurements of negative quadrupole alignments at low collision energies for high-J states could be used to affirm the picture of reaction dynamics presented here.

Note that the J=2 initial state also exhibits negative alignments for low collision energies. The J=2 state gives rise to little trapping, so these alignments point to a preference for reaction of the cartwheel state in direct reaction. Such a preference is often seen in activated reactions at low collision energies and arises because the anisotropy of the PES is generally large in the polar angle, leading to enhanced reaction due to rotational deexcitation of rotational states with low $|m_J|$.[39,52]

This is also the likely cause in this case: the (J=2, m_J=0) state can deexcite, freeing some energy to overcome any low barriers encountered. In addition, the (J=2, m_J=2) state is more tilted with respect to the surface plane than helicopter states for higher J. Helicoptering molecules for J=2 are thus less favorably aligned to react than they are for higher initial rotational states.

3. m_J evolution

We have already shown that the angular momentum quantum number J is largely conserved for rotationally hot molecules, at least up until the point of dissociation. The torques exerted by the interaction with the surface are not sufficient to slow the rotation but may be capable of reorienting it. By monitoring the time evolution of the m_J state, we can establish if the potential can effect changes in the rotational orientation of molecules.

In Fig. 12 we give the probability distribution of m_J at five different times for indirectly reacting molecules initiated in the (J=8, m_J=0) state. The distributions are normalized to the total number of the indirect reacting molecules, so the integral of the area under the distribution tends to decrease in time as molecules react. The figure clearly shows that the trapped molecules are capable of populating m_J states other than the initial m_J. As time progresses, the distribution spreads while retaining its peak at m_J=0. At 30 000 and 40 000 a.u. the distribution has become very broad, though in-plane rotation is still unfavorable, as witnessed by the low probabilities seen for $|m_J|>6$. The directional forces inside the trapping region are obviously sufficient to influence the m_J state, though they cannot significantly impact the J quantum number.

C. Comparison with experiments

In a previous publication we directly compared our results for J=0 with the sticking probabilities measured by Hayden and co-workers for H_2 dissociating on Pt(533), finding good agreement.[12] However, the beam used in experiments typically includes a mixture of rotational states, and–for normal hydrogen—75% of molecules occupy odd-J states and only 25% even-J states.

To make our results more suitable for comparison with experiment, we have produced orientationally averaged sticking probabilities designed to simulate a molecular beam at various temperatures. Unfortunately, including both even- and odd-J states the results do not exhibit the inverse dependence of reaction on collision energy so characteristic of the experimental data and the calculated results for J=0. The problem has been traced to the reaction probabilities calculated for the J=1 state. The unphysical deexcitation permitted in the classical system (see the discussion in Sec. II B) produces a quenching of trapping for the J=1 molecules and a dropping of the reaction probability at low energies. If quantum dynamics calculations were performed we would expect the J=1 molecules to become trapped in the same way as J=0 molecules, and the J=1 reaction probability curve to look much more like that of J=0 than it does in Fig. 1(a).

Given the problems associated with the J=1 state it seems reasonable to only include even-J states in the beam simulation. We have performed these calculations for a variety of different beam temperatures. In all reasonable cases, the reaction probability curve is virtually unchanged from that for J=0 and therefore qualitatively agrees with experiment. The beam-simulation results are thus not presented here, and the reader is instead referred to the results for the J=0 state.[12]

IV. CONCLUSIONS

We have presented the first study of rotational effects in the reaction dynamics of the dissociation of H_2 molecules on a stepped metallic surface, Pt(211), utilizing an accurate 6D DFT PES. Classical trajectory calculations showed that the dissociation probability depends strongly on the initial rotational state. Slowly rotating molecules (J=1, 2) do not exhibit the enhancement of reaction at low collision energies that characterizes the rotational ground state. The rotational energy quenches the trapping responsible for the indirect reaction mechanism that gives rise to the enhancement.

For fast-rotating molecules (J=6–12), the indirect mechanism becomes active again, enhancing reactivity at

low collision energies. However, this does not involve any energy transfer to rotation, as it is does for $J=0$; energy is only transferred to the translational degrees of freedom parallel to the surface. The difference between the time scales of rotation and translation for such rotational states is such that potential coupling is negligible, and trapped molecules do not change rotational J state.

Degeneracy-resolved calculations showed that trapping is more likely to occur for molecules rotating out of the surface plane than those rotating in plane. Cartwheeling molecules, in particular, have a higher probability of becoming trapped and are more likely to react once trapped. These findings were related to aspects of the PES and interpreted using orientationally averaged potentials. The preference for indirect reaction of molecules rotating out of the surface plane leads to a negative quadrupole alignment at low collision energies. Experimental confirmation of this finding would add strong support to the picture of reaction built up here.

Other aspects of reaction can be attributed to well-documented effects, which are also seen on flat surfaces. For example, adiabatic transfer of energy from rotation to the bond stretch is very effective for high-J initial states, enhancing reactivity at all collision energies. Also, molecules slowly rotating out of the surface plane undergo rotational hindering, causing the reaction probability to drop slightly with J.

ACKNOWLEDGMENTS

We gratefully acknowledge the European Community's Human Potential Programme under Contract No. HPRN-CT-2002-00170 "Predicting Catalysis," and the National Research School Combination "Catalysis Controlled by Chemical Design" (NRSC-Catalysis). We thank G. J. Kroes and S. Stolte for their precious comments and suggestions.

[1] J. T. Yates, J. Vac. Sci. Technol. A **13**, 1359 (1995).
[2] C. R. Henry, Surf. Sci. Rep. **31**, 235 (1998).
[3] T. Zambelli, J. Wintterlin, J. Trost, and G. Ertl, Science **273**, 1688 (1996).
[4] B. E. Nieuwenhuys, Adv. Catal. **44**, 259 (2000).
[5] G. A. Somorjai, J. Phys. Chem. B **106**, 9201 (2002).
[6] S. L. Bernasek and G. A. Somorjai, J. Chem. Phys. **62**, 3149 (1975).
[7] I. E. Wachs and R. J. Madix, Surf. Sci. **58**, 590 (1976).
[8] K. Christmann and G. Ertl, Surf. Sci. **60**, 365 (1976).
[9] A. T. Gee, B. E. Hayden, C. Mormiche, and T. S. Nunney, J. Chem. Phys. **112**, 7660 (2000).
[10] A. T. Gee, B. E. Hayden, C. Mormiche, and T. S. Nunney, Surf. Sci. **512**, 165 (2002).
[11] R. A. Olsen, D. A. McCormack, and E. J. Baerends, Surf. Sci. **571**, L325 (2005).
[12] D. A. McCormack, R. A. Olsen, and E. J. Baerends, J. Chem. Phys. **122**, 194708 (2005).
[13] M. Beutl, M. Riedler, and K. D. Rendulic, Chem. Phys. Lett. **247**, 249 (1995).
[14] E. Watts and G. O. Sitz, J. Chem. Phys. **111**, 9791 (1999).
[15] H. F. Busnengo, W. Dong, P. Sautet, and A. Salin, Phys. Rev. Lett. **87**, 127601 (2001).
[16] H. F. Busnengo, E. Pijper, G. J. Kroes, and A. Salin, J. Chem. Phys. **119**, 12553 (2003).
[17] R. T. van Willigen, M. F. Somers, H. F. Busnengo, and G. J. Kroes, Chem. Phys. Lett. **393**, 166 (2004).
[18] G. te Velde and E. J. Baerends, Phys. Rev. B **44**, 7888 (1991).
[19] G. te Velde and E. J. Baerends, J. Comput. Phys. **99**, 84 (1992).
[20] A. D. Becke, Phys. Rev. A **38**, 3098 (1988).
[21] J. P. Perdew, Phys. Rev. B **33**, 8822 (1986).
[22] R. A. Olsen, Ş. C. Bădescu, S. C. Ying, and E. J. Baerends, J. Chem. Phys. **120**, 11852 (2004).
[23] P. Fouquet, R. A. Olsen, and E. J. Baerends, J. Chem. Phys. **119**, 509 (2003).
[24] R. A. Olsen, P. H. T. Philipsen, and E. J. Baerends, J. Chem. Phys. **119**, 4522 (2003).
[25] H. F. Busnengo, A. Salin, and W. Dong, J. Chem. Phys. **112**, 7641 (2000).
[26] R. A. Olsen, H. F. Busnengo, A. Salin, M. F. Somers, G. J. Kroes, and E. J. Baerends, J. Chem. Phys. **116**, 3841 (2002).
[27] G. Kresse, Phys. Rev. B **62**, 8295 (2000).
[28] M. A. Di Cesare, H. F. Busnengo, W. Dong, and A. Salin, J. Chem. Phys. **118**, 11226 (2003).
[29] M. Luppi, R. A. Olsen, and E. J. Baerends, Phys. Chem. Chem. Phys. (submitted).
[30] P. Riviere, H. Busnengo, and F. Martin, J. Chem. Phys. **121**, 751 (2004).
[31] D. A. McCormack and G. J. Kroes, Chem. Phys. Lett. **296**, 515 (1998).
[32] D. A. McCormack and G. J. Kroes, Phys. Chem. Chem. Phys. **1**, 1359 (1999).
[33] Z. S. Wang, G. R. Darling, and S. Holloway, Surf. Sci. **458**, 63 (2000).
[34] Z. S. Wang, G. R. Darling, and S. Holloway, Surf. Sci. **504**, 66 (2002).
[35] S. Holloway, S. Kay, and G. R. Darling, Faraday Discuss. **105**, 209 (1996).
[36] A. Gross and M. Scheffler, Phys. Rev. B **57**, 2493 (1998).
[37] G. R. Darling and S. Holloway, J. Chem. Phys. **101**, 3268 (1994).
[38] J. Q. Dai and J. C. Light, J. Chem. Phys. **108**, 7816 (1998).
[39] M. F. Somers, D. A. McCormack, G. J. Kroes, R. A. Olsen, E. J. Baerends, and R. C. Mowrey, J. Chem. Phys. **117**, 6673 (2002).
[40] H. A. Michelsen, C. T. Rettner, and D. J. Auerbach, Phys. Rev. Lett. **69**, 2678 (1992).
[41] H. A. Michelsen, C. T. Rettner, D. J. Auerbach, and R. N. Zare, J. Chem. Phys. **98**, 8294 (1993).
[42] C. T. Rettner, H. A. Michelsen, and D. J. Auerbach, J. Chem. Phys. **102**, 4625 (1995).
[43] J. Dai and J. Z. H. Zhang, J. Chem. Phys. **102**, 6280 (1995).
[44] K. Svensson, L. Bengtsson, J. Bellman, M. Hassel, M. Persson, and S. Andersson, Phys. Rev. Lett. **83**, 124 (1999).
[45] B. C. Stipe, M. A. Rezaei, and W. Ho, Science **279**, 1907 (1998).
[46] J. K. Gimzewski, C. Joachim, R. R. Schlittler, V. Langlais, H. Tang, and I. Johannsen, Science **281**, 531 (1998).
[47] J. K. Gimzewski and C. Joachim, Science **283**, 1683 (1999).
[48] A. Yazdani and C. M. Lieber, Nature (London) **401**, 227 (1999).
[49] C. Joachim, J. K. Gimzewski, and A. Aviram, Nature (London) **408**, 541 (2000).
[50] W. Ho, J. Chem. Phys. **117**, 1103 (2002).
[51] H. Hou, S. J. Gulding, C. T. Rettner, A. M. Wodtke, and D. J. Auerbach, Science **277**, 80 (1997).
[52] W. A. Diño, H. Kasai, and A. Okiji, J. Phys. Soc. Jpn. **67**, 1517 (1998).